STATENS GEOTEKNISKA INSTITUT

SWEDISH GEOTECHNICAL INSTITUTE

No. 3

SÄRTRYCK OCH PRELIMINÄRA RAPPORTER

REPRINTS AND PRELIMINARY REPORTS

Supplement to the "Proceedings" and "Meddelanden" of the Institute

Contributions to the Fifth International Conference on Soil Mechanics and Foundation Engineering, Paris 1961.

Part I.

1. Research on the Texture of Granular Masses
   by T. Kallstenius and W. Bergau
2. Relationship between Apparent Angle of Friction – with Effective Stresses as Parameters – in Drained and in Consolidated-Undrained Triaxial Tests on Saturated Clay. Normally-Consolidated Clay
   by S. Odenstad
3. Development of two Modern Continuous Sounding Methods
   by T. Kallstenius
4. In Situ Determination of Horizontal Ground Movements
   by T. Kallstenius and W. Bergau

Reprinted from the Proceedings of the Fifth International Conference on Soil Mechanics and Foundation Engineering, Paris 1961.

STOCKHOLM 1961

Preface

The Swedish Geotechnical Institute here presents four reports from the "Proceedings of the 5th International Conference on Soil Mechanies and Foundation Engineering", 1961, prepared by officers of the Institute. The papers contain a statistical and experimental study of the behaviour of granular materials and a mathematical approach to the shearing resistance of clay. Moreover, a description is given of some Swedish sounding equipment and inclinometers and the results obtained with them.

A limited number of copies of these reprints is being issued as exchange matter and for distribution to institutions and others on our mailing list who did not attend the above conference.

Stockholm, October, 1961

SWEDISH GEOTECHNICAL INSTITUTE

Research on the Texture of Granular Masses

Étude sur la texture des substances granulées

by Torsten KALLSTENIUS, Techn. Lic., Head of Mechanical Department
and
Werner BERGAU, Dr. Ing., Head of Measuring Section, Swedish Geotechnical Institute

Summary

The authors consider that the nature of granular masses is not properly taken into account when calculating their mechanical behaviour; as part of a wider research programme, they have investigated the texture of masses of glass balls.

This texture was studied layer by layer, applying a tetrahedral lattice based on the spacing of the balls, from which the shapes of the tetrahedra were evaluated. The balls were allowed to fall freely under the action of gravity and the base plane was horizontal. Both theory and practical tests prove that there is a tendency for the balls to arrange themselves in "chains", and the number of balls per horizontal unit area is found to be nearly constant in all layers. If this number is deliberately changed in one layer, it will be repeated again after a few more layers.

It was also discovered that the mass is anisotropic to the extent that the height of each tetrahedron is less than required for isotropy. Close to a plane boundary surface the balls arrange themselves in a definite manner for six or ten layers thereby producing a "wall effect". This must be taken into account in laboratory tests.

Sommaire

Dans la détermination habituelle du comportement mécanique des substances granulées, on n'accorde pas, suivant l'opinion des auteurs, une attention suffisante à la nature de ces substances. C'est pourquoi, dans le cadre d'un programme de recherches plus vastes, ils ont étudié la texture de masses de billes de verre.

Cette texture a été étudiée couche par couche et rapportée à une structure tétraedrique basée sur les centres des billes. La forme de ces tétraèdres a été étudiée. On a fait tomber les billes une par une, sous la seule action de la pesanteur. Le fond du récipient était horizontal.

La théorie et les essais montrent, tous deux, que les billes ont tendance à se disposer en « chaînes ». Le nombre des billes par unité de surface horizontale fut trouvé presque constant dans toutes les couches. Si ce nombre est modifié à dessein, dans une couche, on retrouve la valeur normale au bout de quelques couches.

On a trouvé aussi que la masse est anisotrope et que la hauteur de chaque tétraèdre est moindre que celle qui correspondrait à l'isotropie.

Près de la surface limite, les billes s'arrangent en couches plus nettes sur une épaisseur de 6 à 10 couches, ce qui produit un « effet de mur » dont on doit tenir compte dans les essais de laboratoire.

Introduction

In connection with soil pressure cell calibrations (S.G.I. Proc. Nº. 12, 1956), the authors felt that there was a need to explain the mechanical behaviour of granular masses with more attention being paid to their true nature than is usually the case. Mr. Justus Osterman, Director of the Swedish Geotechnical Institute, and the authors have collaborated in an extensive, but yet incomplete, study of these matters (cf. J. Osterman, Some aspects on the properties of granular masses, Svenska Nationalföreningen för Mekanik, Reologisektionen, Meddelande 1, 1959).

It has been common practice, when trying to base calculations on the texture of a granular mass, to assume regular patterns of spheres. It is not possible here to mention all authors, but Bullets "Traité d'Architecture-Pratique" (1691) seems to have been one of the first known. Even a brief consideration indicates, however, that regularity is quite improbable under natural conditions. Nevertheless, masses built up from grains of similar size and approximately spherical shape may be found in nature. Experiments with lead shot by W.O. Smith, P.D. Foote and P.F. Busang (Physical Review, Vol. 34, 1929) may be mentioned here. The authors started with a study of the texture of a mass built up of approximately equally large spheres, under conditions similar to slow sedimentation.

They considered a plane horizontal surface with spherical grains falling freely on to that surface. As far as the grains can hit the surface directly, without touching other grains, distances between grains can be assumed to depend entirely on chance. On the other hand, if they touch grains they will be guided sideways and assume positions where interaction between grains plays an important role.

When so many grains have reached the base plane that no other grain can reach this, the base layer is complete. The grain pattern in this layer can be described if triangles are formed between the centres of the grains. Triangles can be formed more or less at will, but there must be a restrictive regulation to the effect that the triangles shall be formed between adjacent grains in the way which best avoids angles greather than 90°. The shortest diagonal between four adjacent grains was therefore chosen. This is based on the consideration that the grains forming the next layer will normally rest on three base-grains each, but cannot find a stable base if the base-grains form a triangle containing an angle greater than 90°.

If the grains have a radius "r" we can call the sides of the base triangles $a{\cdot}r$, $b{\cdot}r$ and $c{\cdot}r$ where "a" always indicates the longest side and "c" the shortest side.

If a triangle forms the base for a fourth grain, the position of this grain is geometrically determinad as its centre will be situated at the distance 2 r from each of the base grain centres. The distance $h{\cdot}r$ from the base triangle can therefore be calculated.

Fig. 1 shows an elementary tetrahedron as determined

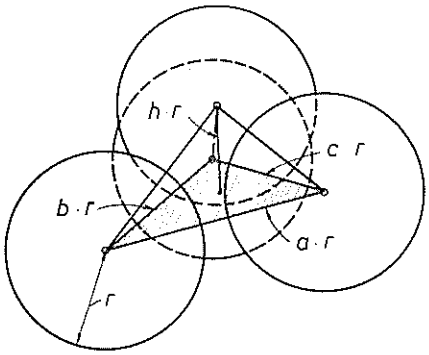

Fig. 1 Elementary Tetrahedron.
Tétraèdre élémentaire.

by coefficients a, b, c and h. The tetrahedra formed by the base layer and the layer immediately above this are called base-tetrahedra. The statistical variation of the dimensions of these base-tetrahedra has been studied by a graphical method. In the granular mass, similar but not identical tetrahedra must exist and the authors have studied them empirically.

Graphical Method

It is not practical to use probability calculations for the texture of the base layer of grains, as the aforementioned interaction effects are complicated. Therefore a combination of graphical solution and calculations has been chosen in order to reach a theoretical understanding.

The interaction of grains may be of two different kinds as illustrated in Fig. 2. Simple interaction occurs when one grain hits another grain and is rolled off in a plane through both grain centres, until both grains remain on the base plane in mutual contact. The distance between the grains is then $2r$, which will determine leg "c" of a base triangle. Double interaction occurs when one grain first hits another grain but is then guided by a third grain to a final position in contact with both grains. Here a triangle is formed where $c = b = 2$. The two types of interaction may combine in chains.

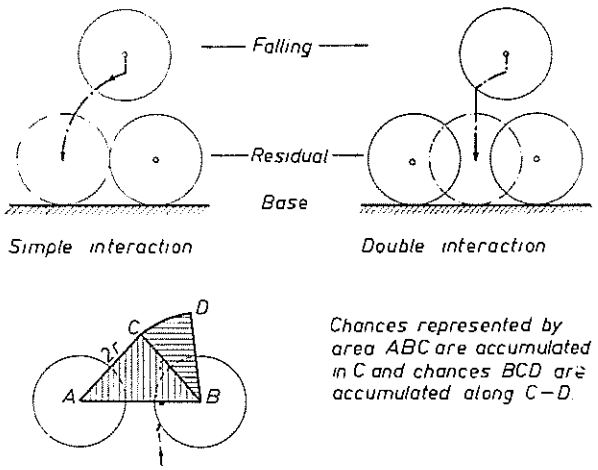

Fig. 2 Interaction between Grains.
Action mutuelle entre les grains.

If we assume the probability to be equal for a grain to reach any part of the base surface, the interaction excepted, we can study the frequency of possible base triangles by dividing the base surface into unit areas and solving the problem graphically. We have chosen a network with a spacing of 0·1 r. Thus our unit area (which represents one chance in our system) is 0·01 r^2.

For each possible unit value of a we studied all possible combinations of b and c but had to consider the following limitations :

(1) $b \leqq a$ due to definition.

(2) $c \leqq b$ due to definition.

(3) $2 \leqq a, b, c$ as no grains can come closer than contact.

(4) Due to definition a fourth grain must not be able to pass the base triangle.

(5) Cases where an angle of the base triangle exceeds 90° cannot be used. Here one must reckon with the chance that a fourth grain will be rolled off to the opposite side of line "a", permitting the formation of two new triangles a_1, b_1, c_1 and a_2, b_2, c_2 (here called redivision).

(6) Due to symmetry only half of the triangles need be checked.

The above limitations are shown graphically in Fig. 3. Fig. 4 shows the basic graphical procedure to determine the number of chances for different combinations of "b" and "c" for the arbitrate a-values 3·6 and 2·6. As stated above triangles with an angle exceeding 90° are not included here. Even if for high a-values the number of chances giving such triangles is comparatively high they are not so frequent in the complete network of the base layer. The reason lies in the aforementioned procedure to select the diagonal between four adjacent grains which produces the minimum possible number of triangles with angles exceeding 90°.

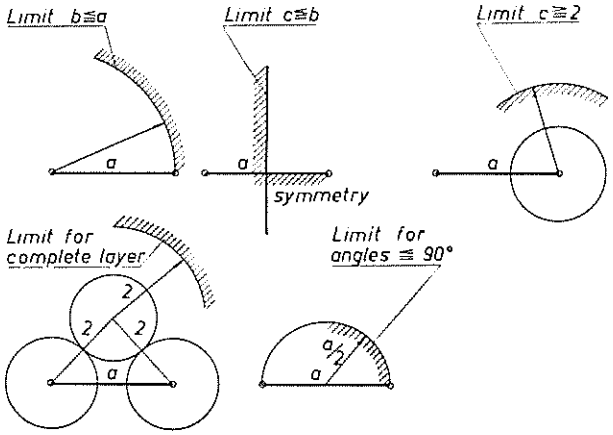

Fig. 3 Limiting Values. (Graphical Evaluation.)
Valeurs limites. (Évaluation graphique.)

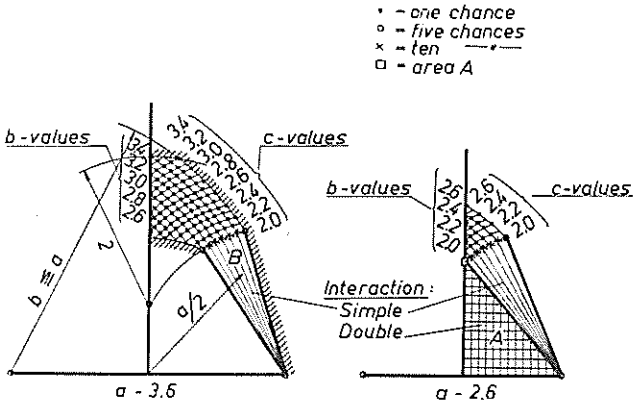

Fig. 4 Determination of Direct and Accumulated Chances.
Détermination de probabilités simples et cumulées.

Fig. 5a illustrates how two triangles ABC and ABD on the common base "a" are redivided by diagonal CD to two other triangles ACD and CBD. As far as D is situated within the area ABE_1, the new triangles contain no angle exceeding 90°. These chances have then already been counted for smaller a-values and nothing new is introduced concerning the base pattern. If D has hit surfaces AD_2D_3 or $BD_6D_5D_4$ we obtain one triangle with all angles smaller than 90° (which has already been counted), and one triangle with an angle exceeding 90° for each unit area. The latter triangles cannot form bases for tetrahedra but will exist in the base pattern between the tetrahedra. The probability for angles exceeding 90° is governed by the ratio between the areas giving such triangles and the total possible area below AB. An important requirement is that no diagonal should exceed "a".

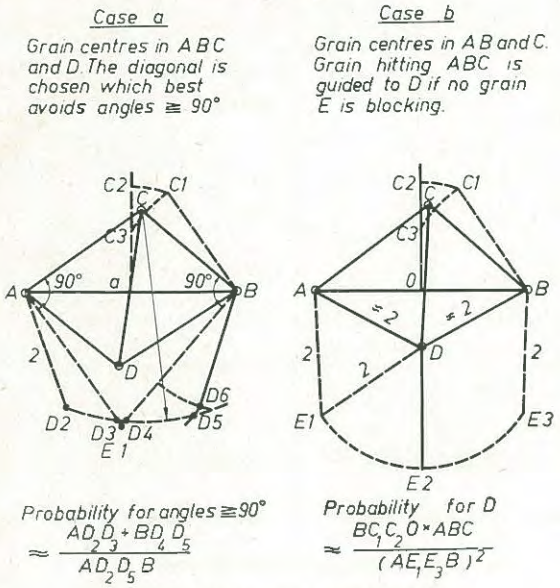

Fig. 5 Redivision of Base Triangles.
Division des triangles de base.

A special effect is demonstrated in Fig. 5b. If a grain hits surface ABC and no grain is present in $AE_1E_2E_3B$, it will be guided by double interaction to a position D. However, it is necessary that grain C reaches its position before a grain hits $AE_1E_2E_3B$ and that a grain then hits surface ABC before a grain hits $AE_1E_2E_3B$, which means two consecutive events and a corresponding small probability. The process means more probability for the formation of triangles ACD and CBD.

Certain special cases with small probability have not been described here although they were considered in our studies.

Frequencies for different combinations of a, b, c and h and their average values have thus been calculated from the individual triangles. In Fig. 6 are given the frequency distributions for the base layer and the base tetrahedra together with measured values from layers 5 and 7 in test B which will be described below.

In Table 1 we have given the frequencies of different constellations of grains in the base layer.

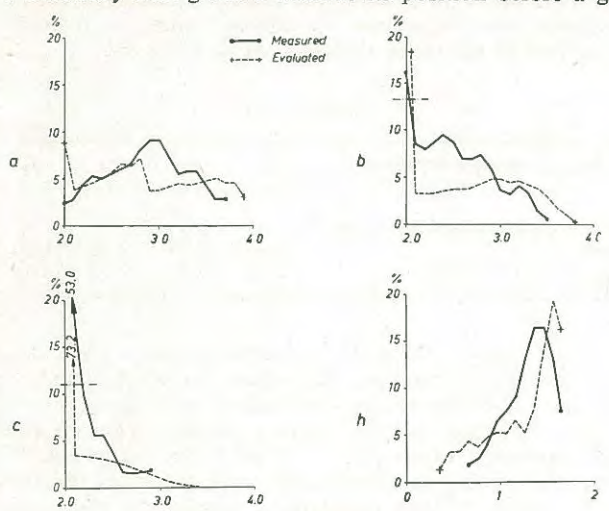

Fig. 6 Frequency Distribution
a b c and h
Distribution de fréquence
a b c et h

Table 1

a-value	*Frequency % Constellations of grains in triangle*			*Reflexion*	*Angles 90°*
	All three free	*One free, two in contact*	*One in contact with two*		
3·9	1·8	1·3	—	—	0·9
3·8	2·7	1·9	—	—	1·1
3·7	2·8	1·8	—	—	1·2
3·6	3·0	2·1	—	—	1·0
3·5	2·8	2·1	—	—	0·9
3·4	2·5	2·1	—	—	0·8
3·3	2·3	2·1	—	—	0·8
3·2	2·0	2·5	—	—	0·6
3·1	1·7	2·5	—	—	0·4
3·0	1·5	2·5	—	—	0·2
2·9	1·2	2·5	—	0·1	0·1
2·8	0·9	2·6	3·8	0·5	—
2·7	0·7	2·3	3·4	0·3	—
2·6	0·5	2·4	3·7	0·8	—
2·5	0·3	1·9	3·5	0·7	—
2·4	0·2	1·3	3·4	0·6	—
2·3	0·1	1·1	3·4	0·6	—
2·2	—	0·7	3·6	0·7	—
2·1	—	0·2	3·6	0·7	—
2·0	—	0·1	8·7	1·8	—
Sum	27·0%	35·9%	37·1%	6·8%	8·0%

There is a great probability of grains coming in contact with each other. The constellation "one in contact with two" means a tendency to form chains. Fig. 7 shows a base layer formed under conditions similar to the assumed and one can there directly see the tendencies indicated in Table 1. As triangles with an angle exceeding 90° cannot form bases for tetrahedra and only about every second triangle of the base layer can be included in a base-tetrahedron, the frequencies for different values of a, b and c will differ in the interspaces from the values given in Fig. 6.

The total number of chances included in this study was about 3100.

Tests

Tests were performed to study the building up of a granular mass, layer by layer.

A glass plate with a layer of glue formed the horizontal base plane. Glass balls with an average diameter of 5·9 mm were dropped carefully on the surface.

Two series of tests, A and B, were performed. Every second

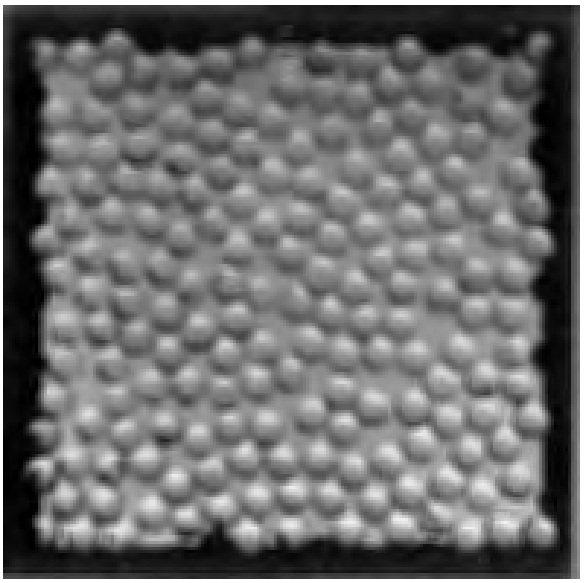

Fig. 7 Base Layer, Test A.
Couche de base, essai A.

layer was uncoloured and every second layer blackened. For each layer the number of balls within a standard area 82 × 82 mm were counted, and the distance of the ball tops to the base plate were measured.

In test *A* the base layer — formed by chance — is shown in Fig. 7. After six layers, balls were poured carefully over the layers to a height of 135 mm above the base plate and two consecutive layers ($n + 1$ and $n + 2$) were counted.

In test *B* the base layer was purposely arranged in the densest possible regular order and seven consecutive layers were counted and measured. The results of the counting are shown in Table 2.

Table 2

Layer	*Number of balls within standard area*	
	Test A	*Test B*
1	180	232
2	184	169
3	176	172
4	168	168
5	183	182
6	184	181
7	—	186
$n + 1$	176	
$n + 2$	185	

We note the nearly equal number of balls for different layers of Test *A* and how the extremely high density of layer 1 in test *B* has been counteraeted by an extra low density in layer 2. After a few layers the numbers counted in test *B* are the same as in test *A*. The influence of chance is constant for the given conditions of formation.

For layers 5 and 7 in test *B* the triangles formed by the ball (grain) centres were measured. The statistical distribution of the measured values *a*, *b* and *c* and the corresponding calculated *h*-values are given in Fig. 6. A comparison with the results of the graphical evaluation of the base layer shows an evident similarity even if the concentration towards small values due to interaction is not as obvious in the test. This should be so, as in layers above the base every grain will be guided by the base grains to a position differing slightly from that selected if the base were a plane surface.

Fig. 8 shows the distribution of grain centre positions above the base surface. The influence of the limiting plane surface has a far-reaching effect and indicates a "wall effect" on the texture of the mass. At a greater distance from the surface the layers begin to mix.

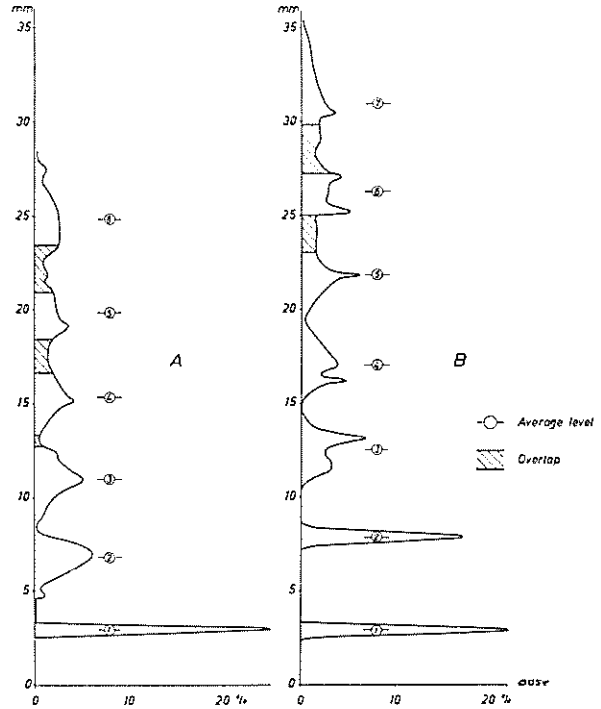

Fig. 8 Distribution of ball centres.
Distributions des centres des billes.

Discussion

The statistical distribution of *a*, *b* and *c*-values and the corresponding *h*-values of the tetrahedra in the mass can be expressed in approximate mathematieal shape but at present the authors prefer to describe the texture by average values. Considering the frequencies of different values *a*, *b* and *c* they arrived at the mean values given in Table 3.

Table 3

Shape of average tetrahedron	a_a	b_a	c_a	h_a
Base tetrahedra, graphical evaluation	2·93	2·59	2·18	1·30
Layers 5 — 7, Test B	2·86	2·53	2·12	1·35

The h_a-values in the table were calculates to suit a_a, b_a and c_a. For a graphical evaluation, the authors have calculated the void ratio "*e*" of the average tetrahedron and found it to be $e = 0{\cdot}51$. This was compared with a calculation for all individual tetrahedra, whieh gave $e = 0{\cdot}50$. It thus seems possible to use the average-tetrahedra for void ratio calculations.

In the course of their calculations, the authors discovered special influences affecting the texture in the mass. As far as the *h*-values are concerned, each triangle of grains can be in contact with one grain on every side, thus forming a pentahedron. When *h* is smaller than unity, pentahedra are no longer

possible which means that the formation of tetrahedra is restricted. h-values smaller than unity must therefore be considered with only half their basic frequency. Therefore the average h-value when calculated for the average values a_a, b_a and c_a is about 0·04 greater than the average h which might be calculated from Fig. 6.

The rather flat shape of the tetrahedra and the fact that the base triangle can only heel little to cause the top grain to roll off (cf. the angle of natural slope as indicated by Fig. 9) leads us to the conclusion that the texture of the mass is un-isotropic (it is not possible to imagine our average tetrahedron standing with its base in a vertical direction). An indication of un-isotropy is the observation in Test A that the number of grains in contact with an area 82 × 82 mm was 179 for a horizontal area but 205 for a vertical area. In this case, however, we were not free from wall effects.

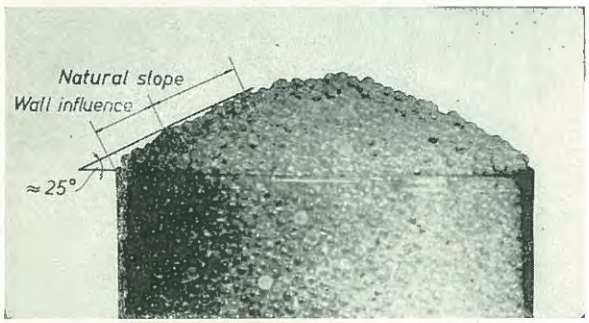

Fig. 9 Angle of natural Slope for Glass Balls.
Angle de talus naturels pour des billes de verre.

This un-isotropic texture may be an explanation of the consolidation-test curve shape. If the mass of tetrahedra is subjected to stress conditions introducing a stress ellipsoid with altered orientation, the structure may stand an alteration only to a limited extent. Above that a breakdown and re-orientation of the structure follows. A direct impression of that is obtained when deforming a mass of billiard balls held together by a net. The authors consider that the orientation of the texture should be allowed for by suitable coefficients when calculations are undertaken.

The authors have studied the influence of wall effects on void ratio determinations. In Test A the average void ratio (including wall disturbances) was found by experiment to be $e = 0{\cdot}61$ in a container measuring 187 × 144 × 130 mm. They determined the void ratios nearest to the limiting surfaces from the measured dimensions of each layer and the counted number of grains. For horizontal surfaces they could check 5 1/2 layers, but for vertical ones only 1 1/2 layers. For the half-layer between the limiting surfaces and the centres of the peripheral grains the void-ratios were very high ($e_h = 1{\cdot}20$; $e_v = 0{\cdot}82$). On the other hand the void ratio in the space between the first and second layers of grain centres was $e = 0{\cdot}41$ for both horizontal and vertical surfaces.

The corrected void ratio for the central mass in Test A was estimated to be $e = 0{\cdot}62$, which is very near the uncorrected value. Figures indicate that the wall-influence may be considerable in relatively smaller vessels (cf. K. SCHUBERT, Einfluss der Versuchszylinderabmessungen auf die lockerste Lagerung rolliger Böden, Zschr. f. Bauwesen, COTTBUS, H.2 1957-1958).

The high void ratio in the outermost half-layer is known to affect permeability tests, and the very dense and ordered next layers form a skin which affects compression tests and strength tests (cf. S.G.I. Proc. No. 12 p. 44, Fig. 28).

The obtained void ratio $e = 0.62$ may be compared with the void ratio calculated from the average tetrahedron in layers 5-7, Test B, which was $e = 0{\cdot}60$.

The tetrahedra seem to be guided by the plane limiting surfaces in such a way that the inter-spaces between the tetrahedra (which need not have tetrahedral shape) are smaller on the average than the tetrahedra. In the mass unaffected by wall effects tetrahedra and interspaces are more equal in volume.

Wall effects are noteworthy in several different respects. The influence on texture as indicated by Fig. 8 seems to have the most far-reaching effect. The influence on void ratio consists of, firstly, one very special limit effect in the half-layer close to a plane surface and secondly, less important changes in the void ratio of the consecutive layers.

Additional Tests

The authors have here dealt with glass balls and one set of building-up formations where every grain was permitted to find an individual stable position. It is difficult to obtain smaller void ratio by simple packing. Penetration tests in similar materials show a great increase in penetration resistance when the same void ratio is approached ($e \approx 0{\cdot}60$). Table 4 shows the void ratios for glass balls, two types of quartz sand and one type of gravel for different conditions of formation (cf. also Kolbuszewski, Proc. 2nd Int. Conf. on Soil Mech. and Foundation Engng., Vol. 1, pp. 158-165).

Table 4

Material	*Tests in ∅ 75 mm glass cylinder*				*Tests in rubber sack*	
	Slowly poured	*Quickly poured*	*Tempered*	*Rolled*	*Atmospheric pressure*	*Vacuum*
∅ 2 mm glass balls	0·59	0·65	0·59	0·70	0·53	0·50
∅ 4 mm glass balls	0·61	0·66	0·61	0·71	0·61	0·51
∅ 6 mm glass balls	0·61	0·66	0·59	0·75	0·60	0·50
Normal Sand A	0·61	0·83	0·59	0·83	0·54	0·51
Normal Sand B	0·68	0·93	0·66	0·93	0·61	0·59
Gravel ∅ 2-4mm	0·63	0·90	0·60	0·92	0·60	0·51

Fig. 10 shows how the texture of a base layer is changed when stresses are introduced in the plane. One can observe a crystalline pattern with amorphous zones between the "crystals". Fig. 11 shows how a similar pattern is formed when putting a granular mass under stress. This external "skin" must influence laboratory tests very much (cf. L.C. GRATON and H.J. FRASER. J. of Geology Vol. 43, Nov.-Dec. 1935).

Fig. 10 Base Layer Subjected to Stresses in the Plane.
Couche de base soumise à des tensions planes.

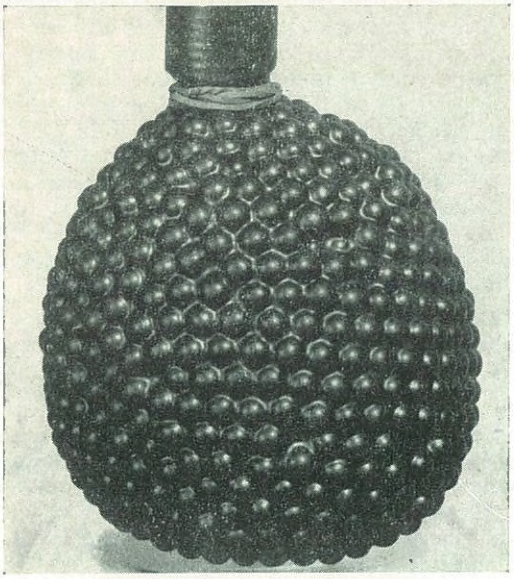

Balls 4 mm
←

Gravel 2-4 mm
→

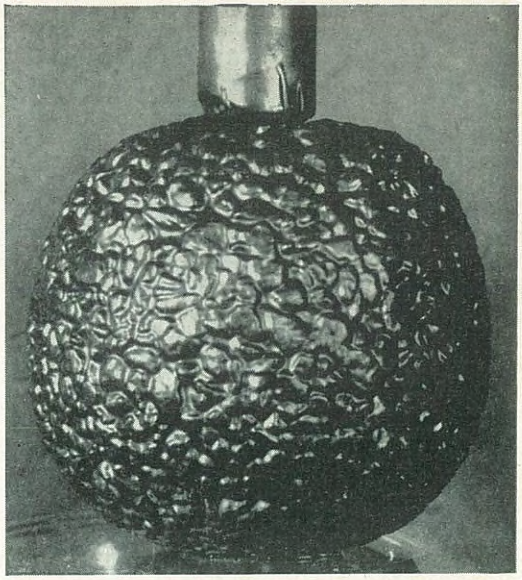

Fig. 11 Skin Effect (Granular Masses under Vacuum).
Effet de peau de substances granulées mises sous vide.

Recapitulating the investigations, it can be said that the idea of examining grain masses both by means of statistical analyses and by experiments seems to the Authors to be a useful attempt to an understanding of the behaviour of granular materials, and may help to avoid experimental errors, for instance due to boundary conditions.

Relationship between Apparent Angle of Friction—with Effective Stresses as Parameters—in Drained and in Consolidated-Undrained Triaxial Tests on Saturated Clay. Normally-Consolidated Clay

Relation entre l'angle de frottement apparent et les contraintes effectives en tant que paramètres — dans des essais triaxiaux drainés et non drainés consolidés sur l'argile saturée : argile normalement consolidée

by S. ODENSTAD, Civil Engineer, Head of Consulting Department Swedish Geotechnical Institute, Stockholm

Summary

When calculating long-term stability of a soil, the shear strength under drained conditions must be known. An adequate triaxial test in the laboratory would then be the drained test. For practical reasons, however, tests on clay must usually be made on consolidated-undrained samples. During the undrained phase, the effective stress then decreases in certain directions in contrast to the behaviour of normally-consolidated clay in nature at drained conditions. Therefore the consolidated-undrained test is not a completely true reproduction of the conditions in the normally-consolidated clay in nature, the stress history being different in the two cases. The author gives a theoretical study of the difference between drained and undrained conditions of normally-consolidated clays.

The shear strength — or shearing stress at the failure surface — in saturated clay may be divided into two parts. One is the true cohesion, which, in theory, is purely a function of the moisture content, and the other is the true friction, corresponding to the true angle of friction. According to the particular stress history, an arbitrary system of effective stresses when acting under drained conditions corresponds to other figures of moisture content and true cohesion than those when acting under undrained conditions. Thus the apparent angle of friction generally is not the same in both cases.

The report shows that in triaxial tests on normally-consolidated clay, the apparent angle of friction is greater in the consolidated-undrained than in the drained test. Finally it is shown how the apparent angle of friction under drained conditions is to be calculated from the data obtained in consolidated-undrained tests ; for this calculation the true angle of friction must be known.

Sommaire

En évaluant la stabilité à long terme il faut connaître la résistance au cisaillement sous des conditions drainées. L'essai triaxial adéquat serait alors l'essai drainé. Pour des raisons pratiques cependant, il faut en général faire, pour ce qui est de l'argile, des essais consolidés non drainés. L'essai non-drainé entraîne une diminution de la contrainte effective dans certaines directions, contrairement à ce qui se passe dans de l'argile normalement consolidée à l'état naturel, dans des conditions non-drainées. L'essai consolidé et non-drainé en laboratoire ne reflète donc pas fidèlement les conditions dans l'argile consolidée normalement à l'état naturel, du fait que le processus de contrainte est différent dans les deux cas. Ce rapport est une étude théorique de la divergence entre les conditions non-drainées et celles drainées de l'argile consolidée normalement.

La résistance au cisaillement — ou l'effort de cisaillement dans la surface de rupture — de l'argile saturée peut se partager en deux parties. L'une des parties est la cohésion vraie qui est la fonction de la seule teneur en eau et l'autre est le frottement vrai correspondant à l'angle vrai de frottement.

Du fait de la différence d'évolution des contraintes la teneur en eau et, partant, la cohésion vraie ont d'autres valeurs lors de l'application d'un système quelconque de contraintes effectives à l'état drainé et à l'état non-drainé. Ceci entraîne que l'angle apparent de frottement n'est généralement pas le même dans les deux cas.

Le rapport démontre que dans les essais triaxiaux sur l'argile consolidée normalement l'angle apparent de frottement est plus grand dans les essais consolidés non drainés que dans ceux drainés. En dernier lieu on montre comment l'angle apparent de frottement dans des conditions drainées doit être évalué en partant des données obtenues dans les essais consolidés non drainés. Pour cette dernière évaluation il faut aussi connaître l'angle vrai de frottement.

Introduction

Osterman has pointed out in (1) that the apparent angle of friction obtained in triaxial tests is often higher in consolidated-undrained tests than in drained tests. He states that the condition can be explained qualitatively by the fact that the true cohesion, which, together with the friction, makes the shearing stress at the failure surface, corresponds to the active effective stresses at the failure in the drained test, while in the consolidated-undrained test it corresponds to the consolidation pressure. The author has calculated the difference between the apparent angles of friction in both types of triaxial tests.

True cohesion

Assume a clay body with a volume and void ratio equal to V_0 and e_0 when the effective stresses are isotropically equal to 0. Consolidation of the clay reduces the volume and the void ratio by ΔV and Δe, and the equation

$$\Delta e = (1 + e_0) \frac{\Delta V}{V_0}$$

becomes valid.

The true cohesion c can be expressed

$$c = k \cdot \Delta e$$

or

$$c = k(1 + e_0)\,\frac{\Delta V}{V_0} \qquad \ldots\ (1)$$

where k is a constant, assumed to be chosen so that the rectilinear relationship between c and Δe gives the best approximation to the actual relationship between c and Δe. The approximate expression gives $c = 0$ for $\Delta V = 0$, i.e. for effective stresses isotropically equal to 0; this seems plausible with normally-consolidated clay.

Drained test

With

σ'_1 = axial effective pressure
σ'_3 = radial effective pressure
E_c = "modulus of elasticity" at compression
μ = Poisson's ratio

the expression

$$\varepsilon_1 = \frac{1}{E_c}(\sigma'_1 - 2\mu\sigma'_3)$$

$$\varepsilon_3 = \frac{1}{E_c}[-\mu\sigma'_1 + (1-\mu)\sigma'_3]$$

is obtained for the unit compressions ε_1 and ε_3, and for the unit reduction of volume $\frac{\Delta V}{V_0}$ the expression

$$\frac{\Delta V}{V_0} = \varepsilon_1 + 2\varepsilon_3 = \frac{1}{E_c}(1 - 2\mu)(\sigma'_1 + 2\sigma'_3)$$

By inserting into Eq. (1) the following expression for the true cohesion c prevailing at the stresses σ'_1 and σ'_3 is obtained

$$c = k(1 + e_0)\cdot\frac{1}{E_c}(1 - 2\mu)(\sigma' + 2\sigma'_3).$$

With

φ = the true angle of friction the failure condition (Fig. 1)

$$\frac{\sigma'_1 - \sigma'_3}{\sigma'_1 + \sigma'_3 + \frac{2}{\mathrm{tg}\varphi}\cdot k(1 + e_0)\cdot\frac{1}{E_c}(1 - 2\mu)(\sigma' + 2\sigma'_3)} = \sin\varphi$$

is valid which is rewritten

$$\frac{\sigma'_1}{\sigma'_3} = \mathrm{tg}^2\left(45 + \frac{\varphi'_d}{2}\right)$$

$$= \frac{1 + \sin\varphi + 4\cos\varphi\cdot k(1 + e_0)\cdot\frac{1}{E_c}(1 - 2\mu)}{1 - \sin\varphi - 2\cos\varphi\cdot k(1 + e_0)\frac{1}{E_c}(1 - 2\mu)} \qquad \ldots\ (2)$$

Mohr's circles of effective stresses at failure have thus a common tangent running through origin. This tangent slopes at the angle φ'_d towards the σ-axis. Eq. (2) shows directly that the apparent angle of friction $\varphi'_d >$ true angle of friction φ.

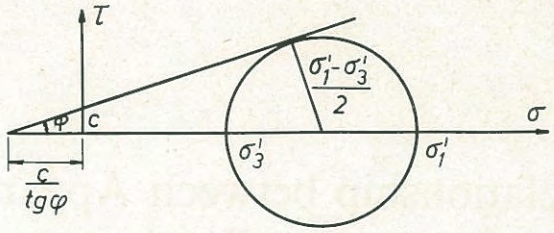

Fig. 1 Effective stresses σ'_1 and σ'_3 at failure. True angle of friction = φ and true cohesion = c.
Contraintes effectives σ'_1 et σ'_3 à la rupture. Angle vrai de frottement = φ et cohésion vraie = c.

Consolidated-undrained test

The sample is first subjected to the isotropically equal consolidation pressure p. While the total pressure often is maintained in a radial direction, the axial pressure is increased till failure occurs. In the undrained phase the following are valid :

σ'_1 = axial effective pressure
σ'_3 = radial effective pressure
$\sigma'_1 - p$ = increase of axial effective pressure from the beginning of the phase
$p - \sigma'_3$ = decrease of radial effective pressure from the beginning of the phase
$p - \sigma'_3$ = neutral pressure

In the undrained phase the unit compression

$$\varepsilon_1 = \frac{\sigma'_1 - p}{E_c} + 2\mu\,\frac{p - \sigma'_3}{E_s}$$

is obtained in axial direction, and in radial direction the unit elongation

$$\varepsilon_3 = (1 - \mu)\,\frac{p - \sigma'_3}{E_s} + \mu\,\frac{\sigma'_1 - p}{E_c}$$

where E_s = modulus of elasticity at swelling.

From the fixed volume condition

$$\varepsilon_1 - 2\varepsilon_3 = 0$$

is obtained

$$\frac{\sigma'_1 - p}{E_c} + 2\mu\,\frac{p - \sigma'_3}{E_s} - 2(1 - \mu)\,\frac{p - \sigma'_3}{E_s} - 2\mu\,\frac{\sigma'_1 - p}{E_c} = 0,$$

whereof with $\lambda = \frac{E_c}{E_s}$,

$$\lambda = \frac{1}{2}\cdot\frac{\sigma'_1 - p}{p - \sigma'_3} \qquad \ldots\ (3)$$

and after rewriting

$$3p = \sigma'_1 + 2\sigma'_3 + 2\,\frac{1 - \lambda}{1 + 2\lambda}(\sigma'_1 - \sigma'_3) \qquad \ldots\ (4)$$

For the unit reduction of volume $\frac{\Delta V}{V_0}$, calculated from the

stressless condition, the expression

$$\frac{\Delta V}{V_0} = \frac{1}{E_c}(1 - 2\mu) \cdot 3p$$

is valid. By inserting into Eq. (1) the following expression for the true cohesion c curing the undrained phase is obtained

$$c = k(1 + e_0) \cdot \frac{1}{E_c}(1 - 2\mu) \cdot 3p$$

which after insertion of Eq. (4) becomes

$$c = k(1 + e_0)\,\frac{1}{E_c}(1 - 2\mu)$$

$$\left[\sigma'_1 + 2\sigma'_3 + 2\frac{1 - \lambda}{1 + 2\lambda}(\sigma'_1 - \sigma'_3)\right].$$

Thus at failure the condition now valid is

$$\frac{\sigma'_1 - \sigma'_3}{\sigma'_1 + \sigma'_3 + \frac{2}{\operatorname{tg}\varphi}\,k(1 + e_0)\frac{1}{E_c}(1 - 2\mu)\left[\sigma'_1 + 2\sigma'_3 + 2\frac{1 - \lambda}{1 + 2\lambda}(\sigma'_1 - \sigma'_3)\right]} = \sin\varphi$$

which is rewritten

$$\frac{\sigma'_1}{\sigma'_3} = \operatorname{tg}^2\left(45 + \frac{\varphi'_u}{2}\right) = \frac{1 + \sin\varphi + \left(1 - \frac{1 - \lambda}{1 + 2\lambda}\right)4 \cdot \cos\varphi \cdot k(1 + e_0) \cdot \frac{1}{E_c}(1 - 2\mu)}{1 - \sin\varphi - \left(1 + 2\frac{1 - \lambda}{1 + 2\lambda}\right)2 \cdot \cos\varphi \cdot k(1 + e_0) \cdot \frac{1}{E_s}(1 - 2\mu)} \quad \ldots\ (5)$$

Mohr's circles of effective stress at failure have thus a common tangent through origin, sloping at the angle φ'_u towards the σ axis. The angle φ'_u is the apparent angle of friction in this type of test.

Comparison between the drained and the consolidated-undrained test

With

$$a = 2\cos\varphi \cdot k(1 + e_0) \cdot \frac{1}{E_c}(1 - 2\mu)$$

inserted into Eqs. (2) and (5) are obtained

$$\operatorname{tg}^2\left(45 + \frac{\varphi'_d}{2}\right) = \frac{1 + \sin\varphi + 2a}{1 - \sin\varphi - a} \quad \ldots\ (6)$$

$$\operatorname{tg}^2\left(45 + \frac{\varphi'_u}{2}\right) = \frac{1 + \sin\varphi + 2a - 2\frac{1 - \lambda}{1 + 2\lambda}a}{1 - \sin\varphi - a - 2\frac{1 - \lambda}{1 + 2\lambda}a} \quad \ldots\ (7)$$

From these equations is obtained the expression

$$\frac{1}{\operatorname{tg}^2\left(45 + \frac{\varphi'_d}{2}\right) - 1} - \frac{1}{\operatorname{tg}^2\left(45 + \frac{\varphi'_u}{2}\right) - 1} = \frac{\left(\frac{3}{1 + 2\lambda} - 1\right)a}{2\sin\varphi + 3a} \quad \ldots\ (8)$$

The value of λ now determine whether φ'_u is greater than, equal to or smaller than φ'_d.

According to Eq. (8) the following relations are valid :

$$\left.\begin{array}{l} \text{at } -\frac{1}{2} < \lambda < 1 \text{ is } \varphi'_u > \varphi'_d \\ \text{at } \lambda = 1 \text{ is } \varphi'_u = \varphi'_d \\ \text{at other values of } \lambda \text{ is } \varphi'_u < \varphi'_d \end{array}\right\} \quad \ldots\ (9)$$

In (2) Skempton gives values that are valid for his pore pressure coefficient A in different clays at the failure phase. In saturated clay the coefficient A expresses the neutral pressure $p - \sigma'_3$ caused by the deviator stress $\sigma'_1 - \sigma'_3$ according to the formula

$$p - \sigma'_3 = A(\sigma'_1 - \sigma'_3)$$

Comparison with Eq. (3) rewritten in the form

$$p - \sigma'_3 = \frac{\sigma'_1 - \sigma'_3}{1 + 2\lambda}$$

shows that transformation from A to λ may be made according to the formula

$$\lambda = \tfrac{1}{2}\left(\frac{1}{A} - 1\right).$$

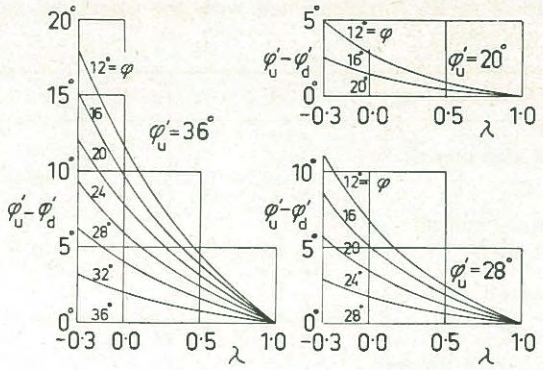

Fig. 2. The correction $\varphi'_u - \varphi'_d$ at various values of φ_u', φ and λ
La correction $\varphi'_u - \varphi'_d$ en fonction de φ'_u, φ et λ.

Skempton's table, complemented with the calculated values of λ is as follows :

Type of clay	*A*	λ
Clays of high sensitivity	$+\frac{3}{4}$ to $+1\frac{1}{2}$	$+\frac{1}{6}$ to $-\frac{1}{6}$
Normally - consolidated clays	$+\frac{1}{2}$ to $+1$	$+\frac{1}{2}$ to 0
Compacted sandy clays	$+\frac{1}{4}$ to $+\frac{3}{4}$	$+\frac{3}{2}$ to $+\frac{1}{6}$
Lightly over-consolidated clays	0 to $+\frac{1}{2}$	$> +\frac{1}{2}$
Compacted clay gravels	$-\frac{1}{4}$ to $+\frac{1}{4}$	$< -\frac{5}{2}$ or $> +\frac{3}{2}$
Heavily over-consolidated clays	$-\frac{1}{2}$ to 0	$< -\frac{3}{2}$

The table and the expressions (9) show now that $\varphi'_u > \varphi'_d$ in normally-consolidated clays and also in highly sensitive clays. The value of φ'_d can now be calculated as follows :

Eq. (7) is rewritten in the form

$$a = \frac{(1 - \sin\varphi)\,\mathrm{tg}^2\left(45 + \frac{\varphi'_u}{2}\right) - 1 - \sin\varphi}{\left(1 + 2\frac{1-\lambda}{1+2\lambda}\right)\mathrm{tg}^2\left(45 + \frac{\varphi'_u}{2}\right) + 2\left(1 - \frac{1-\lambda}{1+2\lambda}\right)} \quad \ldots\ (7a)$$

From the consolidated-undrained test are obtained φ'_u and, by Eq. (3), λ. The true angle of friction φ is determined by special tests. Insertion into (Eq. (7a) gives the value of a and by insertion into Eq. (6) finally, the required value of φ'_d is obtained. The result is shown in Fig. 2.

References

[1] OSTERMAN, J. (1960). Notes on the shearing resistance of soft clays. *Acta Polytechnica Scandinavica*, Ci2, Stockholm.

[2] SKEMPTON, A. W. (1954). The pore-pressure coefficients A and B. *Géotechnique*, 4 : 4 :, pp. 143-147.

Development of two Modern Continuous Sounding Methods

Deux méthodes modernes de sondage continu. Interprétation des résultats

by T. KALLSTENIUS, Techn. lic., Head of Mechanical Department, Swedish Geotechnical Institute

Summary

For more than ten years the Swedish Geotechnical Institute has used two sounding devices — the Iskymeter and the Sounding Machine — which differ from most others in that they produce continuous records ready for immediate interpretation.

The methods were radically different from the standard Swedish sounding practice and therefore time was needed to calibrate them and to gather experience. In recent years they have been widely and successfully used, especially in connection with investigations of stability conditions in the Göta River Valley in southwestern Sweden and the publication of some experience gained seems to be justified.

The Iskymeter works mainly in clay and gives shear strength data agreeing with the results of other rapid tests. The Sounding Machine is used to distinguish the soil strata and to determine their thickness and homogeneity.

When evaluating a large number of diagrams, simplified evaluation methods are necessary, but also such evaluation can yield essential information as to the ground conditions over large areas.

The continuous records enable reliable statistical evaluation to be made and permit the selection of typical layers for sampling. This procedure makes for a great reduction in the quantity of samples required and considerable savings in field work, drawing office costs and laboratory work, reducing guesswork considerably. Thus the overall economy is very good. Even the cost per metre of depth sounded is low.

Sommaire

Depuis plus de dix ans l'Institut Suédois de Géotechnique emploie deux appareils de sondage — « l'Iskymètre » et la sondeuse — qui diffèrent de la plupart des autres appareils en ce qu'ils fournissent des enregistrements continus immédiatement interprétables.

Les méthodes employées diffèrent radicalement de la pratique de sondage suédoise normale, et de ce fait il a fallu du temps pour les mettre au point et pour acquérir de l'expérience. Pendant ces dernières années elles ont été employées fréquemment et avec succès, notamment au cours de la recherche des conditions de stabilité du sol dans la vallée du fleuve Göta dans le sud-ouest de la Suède et la publication de l'expérience ainsi acquise nous a paru justifiée.

Suit une description sommaire des méthodes de l'interprétation des résultats. L'iskymètre travaille principalement dans l'argile et fournit des valeurs de la résistance au cisaillement concordant avec les résultats d'autres essais rapides. La sondeuse est utilisée pour distinguer les différentes couches du sol, pour déterminer leur épaisseur et pour apprécier leur homogénéité.

Pour l'interprétation d'un grand nombre de diagrammes, il est nécessaire d'avoir recours à des méthodes simplifiées, mais aussi une telle interprétation peut fournir des renseignements essentiels sur les caractéristiques du sol dans de vastes étendues.

Les enregistrements continus permettent une interprétation statistique très sûre et autorisent le choix de couches caractéristiques dans lesquelles seront prélevés des échantillons. Cette méthode permet une réduction importante du nombre des échantillons nécessaires et des économies considérables à la fois sur les opérations sur le terrain, les dessins et les essais de laboratoire. En outre, elle réduit considérablement les incertitudes. L'économie générale de l'opération est ainsi excellente. Les frais par mètre de sondage sont modiques.

Introduction

Mr. W. Kjellman — first head of the Swedish Geotechnical Institute — wished to develop sounding methods which were quicker and cheaper and even less dependent on human factors than simple manual sounding. During the years 1938-1942, assisted by Mr. Y. Liljedahl, he developed the prototype of a machine — now called Iskymeter — (Royal Swedish Institute for Engineering Research Proc. No. 170, Walter Kjellman, En metod att direkt i marken bestämma jordlagrens skärhållfasthet). The Author has now developed the iskymeter to its present form and has also developed another machine, the sounding machine (utilizing a principle of eliminating skin-friction given by W. KJELLMAN, cf. Statens Geotekniska Institut, *Medd.* Nr 2 1949).

The SGI Sounding machine

Principles—The machine (Fig. 1) was developed mainly for large area sounding and was intended to be an improvement of the Swedish Standard sounding method (Cf. GEOTECHNICAL COMMISSION. Swedish State Railways, *Final report*, 1922).

The machine uses a conical point fastened to a rotating rod, pushed by means of two rollers, pressed hard against the sounding rod. The rollers are mounted in a rotor. The rate between rotation and push is kept constant.

Power is provided by an hydraulic motor mounted on a pivot. This swings on a vertical axis and is supported by the rotor. Pivot and rotor are free to move upwards and downwards and are carried by a set of helical springs. When an axial force is developed in the sounding rod the system is lifted proportionally to the force. The reaction in a tangential direction when driving the rotor is taken by a horizontal spring.

An arm fixed on the pivot moves upwards when penetration resistance increases and in a horizontal direction when the turning force increases. Disturbance from friction or from the hose supplying the hydraulic fluid joined near the centre of rotation are normally small.

The horizontal and vertical movement of the arm influence a pen recording on a waxed paper. A vertical load of 100 kg gives a deflexion of 10 mm on the chart (Total range 1 000 kg).

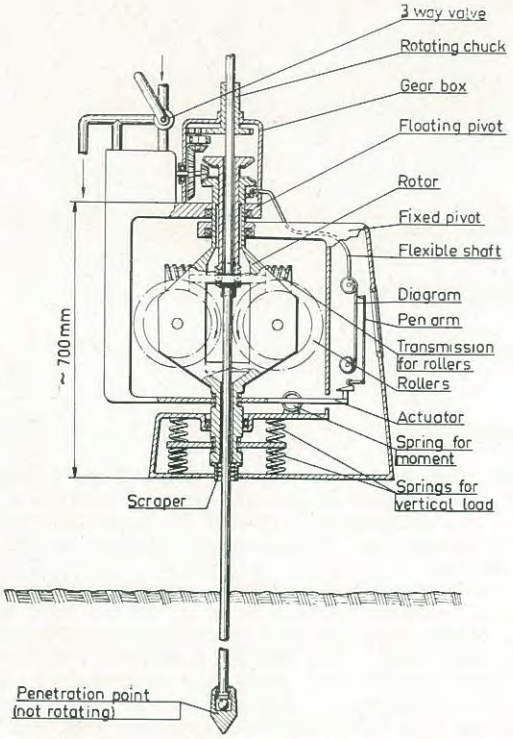

Fig. 1 General arrangement of SGI sounding machine.
Machine de sondage type SGI.

The paper is moved by the rotor over a flexible shaft (1 m of penetration corresponds to a paper travel of 10 mm).

Fig. 2 shows how skin friction is eliminated. As there is a constant relationship between penetration and rotation, the direction of travel of each surface element of the sounding rod is known. The moment required to turn the rod is measured. If the rod turns around its centre an estimate of the horizontal force can be made. Moreover it can be assumed that the frictional force (F) on any surface element will be directed opposite to the travel. The frictional force consists of one horizontal part (F_h) (already calculated from the turning moment) and one vertical part (F_v) in constant relationship to the known horizontal part. Thus, the turning moment is proportional to the vertical part of the skin friction and can be introduced as an automatic correction on the recorded total vertical force (V). This is done by a sloping curve on the actuator-arm.

The sounding rods are coupled automatically by means of a rotating chuck which makes continuous penetration possible.

Calibrations—Static calibrations have shown that with loads of 0-500 kg and moments from 0-18 kgm, the correction on the measured vertical load is normally smaller than 10 kg. A suitable correction can be made where required.

The method of using the turning moment for the elimination of skin friction has been checked by surrounding the sounding rod with a tube where sand could be put under pressure. The calibrations showed that the way to eliminate skin friction is substantially correct if a correction on point resistance of — 2·5 kg per kgm turning moment is made. In very soft clay with a rotating point of the same diameter as the sounding rods, the author found that the machine recorded only the weight of the rod as intended. (The correction in kg for rod weight is + 2·47 h, where h is sounding depth in metres).

This correction for skin friction will not apply if the rotor is accelerated or retarded or if the couplings of the sounding rod are not quite concentric, or if the rods are not quite straight. This may only occasionally introduce errors which ought to be considered.

More serious errors are introduced by varying static pressure in the bore-hole. The author has used three different point diameters, namely 25 mm, 40 mm and 80 mm (the latter is not used any more), in combination with a 20 mm sounding rod. The pressure from above on the point (Fig. 3) gives a force dependent on conditions in the ground. We can imagine a vacuum acting above the point. In an open hole we will have the atmospheric pressure. If the hole is filled with water or clay mud with volume weight γ we have a pressure of $h \cdot \gamma$ above the point. Finally, we may have passed through layers of sand with high artesian pressure which may act on the point if the hole is closed above the sand. The possible magnitude of static influences depends on the size of the ring-shaped area accessible for pressure variations. For the 25 mm diameter point this area is only 1·76 sq. cm and disturbance is negligible. For the 40 mm diameter point area is 9·41 sq. cm and disturbance must be considered. It may be an advantage to use the 40 mm diameter point to shallow depths owing to the heavier point resistance and the lower influence of mechanical errors.

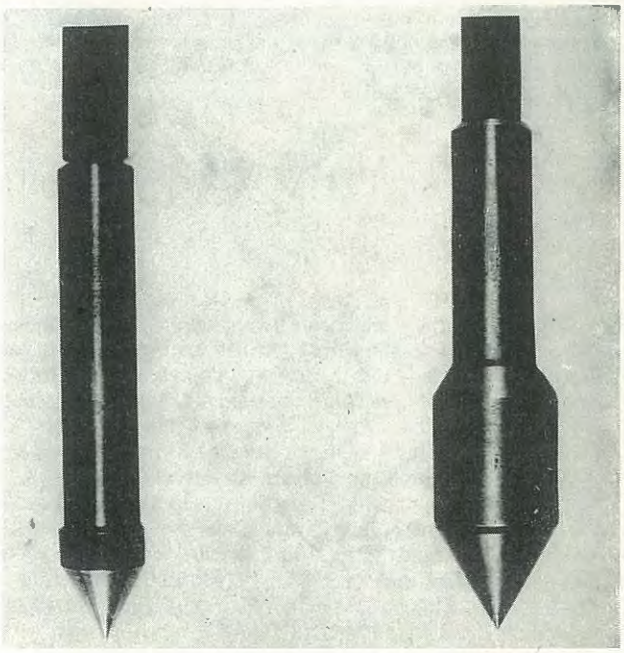

Fig. 3 Points of 25 mm and 40 mm diameter.
Pointes de 25 mm et de 40 mm de diamètre.

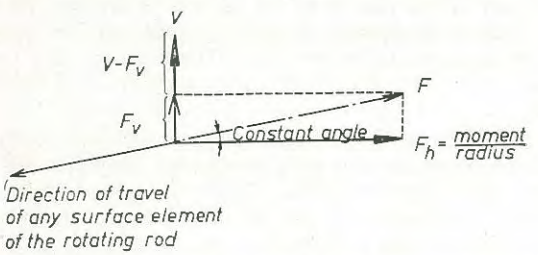

Fig. 2 Principle of separating skin friction from point resistance.
Principe de la séparation du frottement latéral de la résistance de pointe.

The sounding machine has been tried in different materials. Fig. 4 shows a rough relationship between a 25 mm diameter point resistance and the degree of packing of different sands.

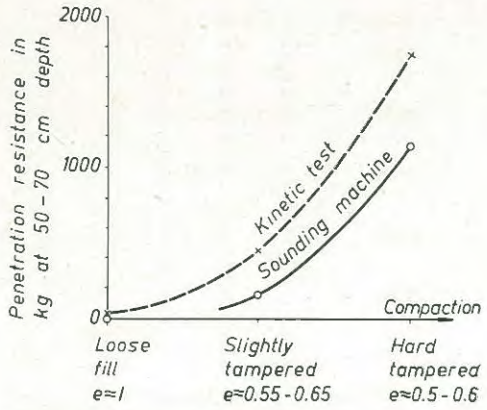

Fig. 4 Resistance of a 25 mm diameter point in sand (Calibration Test).
Résistance de pointe de 25 mm de diamètre dans le sable (Essai d'étalonnage).

The machine has given lower resistance values than a static test, probably because the rod rotates. The influence of a rotative point must be considered to allow for a possibly defective ball bearing. According to tests this reduces point resistance still more but it may also increase penetration. For sand which ranges from normal to dense packing, the machine with the 25 mm diameter point combines adequate reaction with good penetration.

In clay points of different sizes, provided with mantles of different lengths, have been tested by the author. Fig. 5 gives a rough estimate of the influence of point diameter and mantle length on the bearing capacity. The *N*-value is defined as point resistance in kilograms divided by the cross-sectional area of the point in sq. cm. times shear strength in kg per sq. cm. The static conditions in the borehole and the friction along the mantle were not considered. Mantle length equal to the diameter is deemed best. If it is too long the sensitivity and soil pressure on the mantle will have a large and varying influence. If it is too short, sliding surfaces around the point may influence point resistance. To check the influence of these conditions the author has poured drilling muds of different specific gravity into the borehole. The drilling mud greatly reduced the measured point-resistance. For an 80 mm diameter point and with a mud weighing 2 kg per litre, point resistance was eliminated. At depths down to 10 to 20 m however, the author has sometimes used *N*-values from 20 to 25 to good advantage for an approximate estimate of clay strength when using points of 40 and 25 mm diameter.

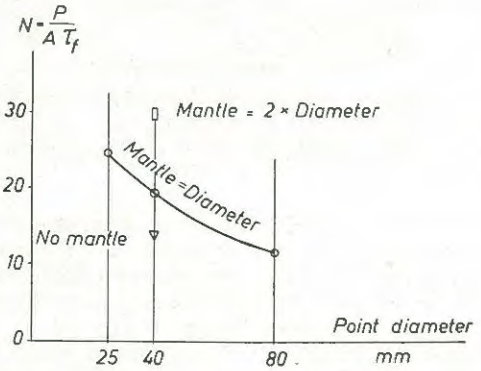

Fig. 5 Point resistance in clay (Approximate Values).
Résistance de pointe dans l'argile (Valeurs approximatives).

Application and Experience—The records of this sounding machine are claimed to give a better indication of soil stratification than alternative sounding methods.

Fig. 6 shows typical curves for clay, sand and gravel of different density. By judging the shape of the curve, the point resistance and the turning moment, sound information can be obtained. A general knowledge of site geology from a continuous core of soil is very helpful as an aid to interpretation.

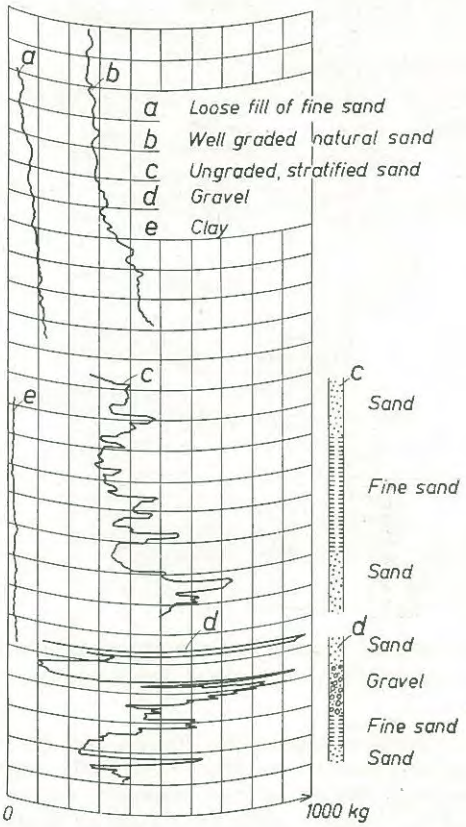

Fig. 6 Typical resistance curves for a point of 25 mm diameter.
Pointe de 25 mm de diamètre. Courbes de résistance caractéristiques.

Fig. 7 shows a curve with notations and interpretation. The operator notes on the diagram direct observations made during sounding. He can hear and feel when the point hits a stone. Bad joints or accelerations and retardations of the rotor influence the records. The operator notes the sounding depth as observed directly on the sounding rods to check possible slip of the rod between the rollers (which happens only occasionally). Moreover, the turning moments are noted at intervals to facilitate interpretation and to enable due allowance to be made for the effect of skin friction.

When using the 25 mm diameter point, the penetration and ability to distinguish sand layers in clay are far better with the sounding machine than with the traditional Swedish sounding apparatus. Near bedrock there are generally typical layers of sand and gravel which can be distinguished on the diagrams and indicate bed-rock. Silty material below the water table may give decreasing point resistance due to increased pore pressure and remoulding caused by the rotating rod.

The capacity of the machine with two operators in Swedish clay is 30 to 50 holes down to 5 to 10 m depth or 10 to 12 holes down to 50 m depth in eight ours, including transport of from 50 to 100 m between the holes.

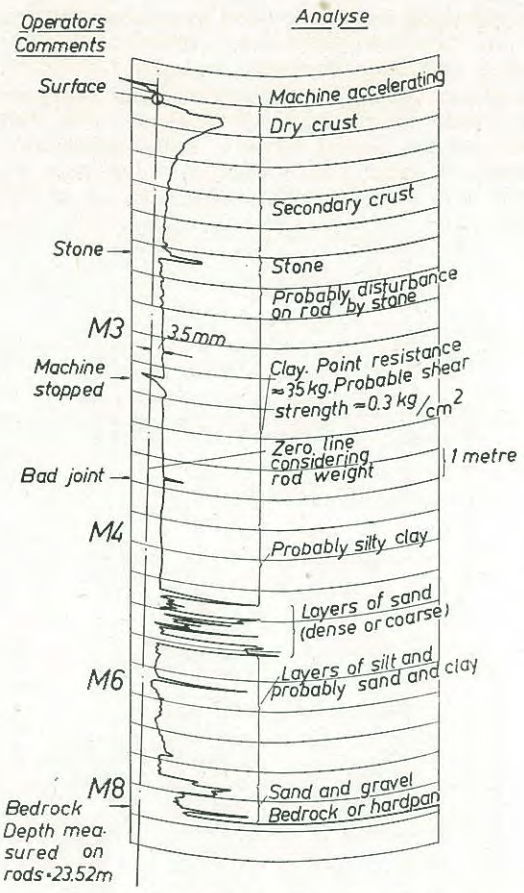

Fig. 7 Analysis of diagram for a point of 25 mm diameter.
Pointe de 25 mm de diamètre. Analyse de diagramme.

A special problem arises when studying the diagrams. If, for instance, this machine produces about 1 000 diagrams in a month, simple tables of the most important values must be prepared. Fig. 8 shows a table for vertical drainage projects where the object is to find permeable layers and the thickness and depth of the clay layers. By plotting point resistances at a certain depth on a map, weak and hard areas can be found (the weak area in Fig. 9 coincided with the lowest part of the ground surface).

With this system points and levels can be selected where a few samples or in-situ tests can give representative values for soil conditions. The sounding machine is cheap in use for jobs exceeding about 200 bored metres or depths below 20 m. It has been used, for example, in Northern Norway for an airfield near Stockholm and in the Göta River Valley in Western Sweden. Rapid setting out of the boreholes is an important factor.

Machine Sounding

Job: K 5552 Sheet: 42

Site: Skå Edeby Point Diameter: 25 mm

Day	Hole	Litt	Total Depth m	Stratification: Dry crust	Clay	Silt or Sand	Resistance at Depth: -5m	-10m	Notations
Line 4775									
58 7/4	1	20625	14,5	0-1,2-4,5	12-5 5,2-13	5-5,2	20	30	Probably stone at -12
	2	20650	32,2	0-0,6-2,5	0,6-20 23-31?	20-2,3 31-32,2	20	30	—
	3	20675	5,2	0	0	0-5,2	—	—	

Fig. 8 Machine sounding data.
Tableau de résultats de sondage fournis par la machine.

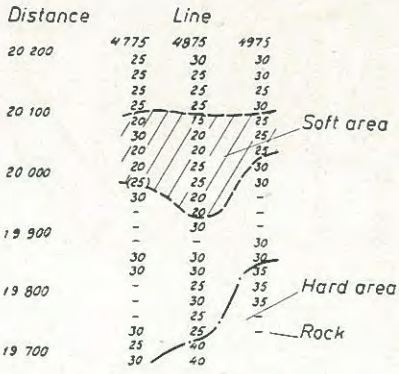

Fig. 9 Plotting of point resistances.
Graphique de la résistance de pointe.

The SGI Iskymeter

Principles—The Iskymeter is intended for sounding mainly in soft ground. Instead of a point, it uses a resistor with foldable wings which is pulled out of the ground. Fig. 10 shows this resistor in different positions, as described. It is pushed down in the soil by means of a rod provided with a special end attachment for the resistor shaft. During thrust into the ground, the wings are folded and the resistor has little resistance and therefore causes only slight disturbance of the soil. When the rod is withdrawn the resistor stays in the ground, and a wire-rope from the resistor ends in a storage-drum on the soil surface. The pushing and withdrawal is normally performed with a separate winch (e.g. the front winch of a lorry).

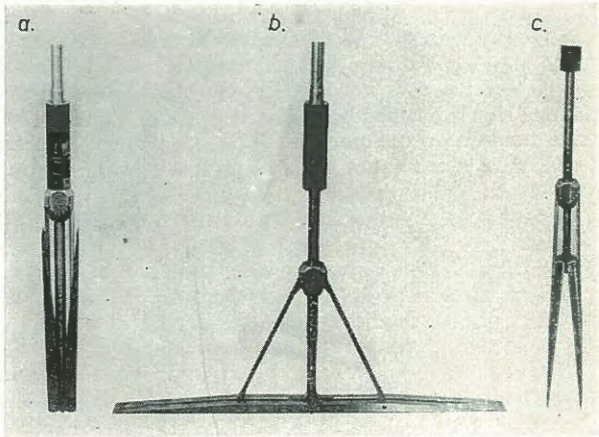

Fig. 10 Resistor for SGI Iskymeter:
(a) installation position;
(b) sounding position;
(c) position when overloaded.
Elément résistant de l'iskymètre type SGI:
(a) position de fonçage;
(b) position de travail;
(c) position de relevage.

The storage-drum is then fastened to a special winch (Fig. 11) which is driven either manually or by means of a small motor, and pulls the resistor out of the ground. During the first 60 cm pull the wings of the resistor-body unfold automatically and assume the position shown in Fig. 10b.

As the wire-rope runs out of the ground it is first cleaned from soil by a special cleaner. Then it bends 90° over a pulley, which is fastened to a lever and torsion beam in such a way that the pulley travels downwards and upwards in direct proportion to the pulling force. This travel is then extended

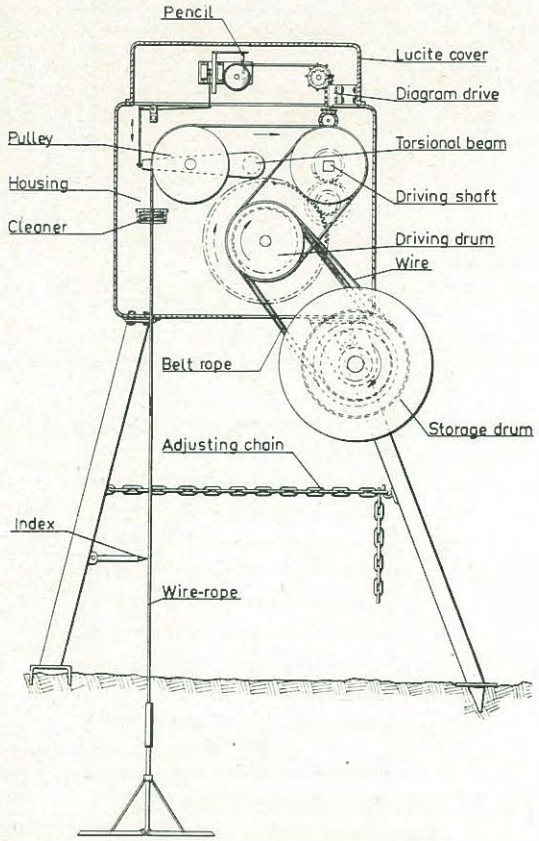

Fig. 11 SGI Iskymeter.
Iskymètre type SGI.

and is used to move a pencil across a paper chart, a pulling force of 1 000 kg giving a pencil travel of 100 mm.

The wire rope is wound around two drums (one of which is driven by the winch) and continues to the storage drum. The rotation of one of the drums is used to move the diagram paper 10 mm for each metre of pull.

Resistors with horizontal cross sectional areas of 200, 100 and 30 sq. cm have been used. If the forces exceed 1 000 kg, a small pin on the resistor shaft breaks and the wings can fold backwards.

The Iskymeter is normally transported on a light trailer but can also be carried by the operating crew between adjacent boreholes.

Calibration—A first calibration of the Iskymeter was performed as early as 1939-1941 by Mr. W. Kjellman and assistants. Fig. 12 shows the relationship between specific vertical pressure on reistors of different cross-section area and shear strengths determined by fall-cone tests. Considerable scatter has been noted.

Influence of sensitivity of the soil and of variations in the pulling speed were suspected as the reasons for this scatter. Mr. B. Jakobson and Mr. O. Wager performed tests with pulling speeds varying from 0·001 to 10 metres per minute. The results indicate dependence on pulling speed and type of material (Fig. 13). Organic matter (which influences e.g. the modulus of elasticity) may also have an influence. At normal speeds (0·50-2·0 m per minute) the influence of speed should be small for a certain material. Fig. 14 shows uncorrected results (as compared with vane tests) from the Göta River Valley. The average scatter was about ± 35 per cent. Both depth and sensitivity have some influence. Mr. J. Osterman, now head of the Swedish Geotechnical Institute, derived

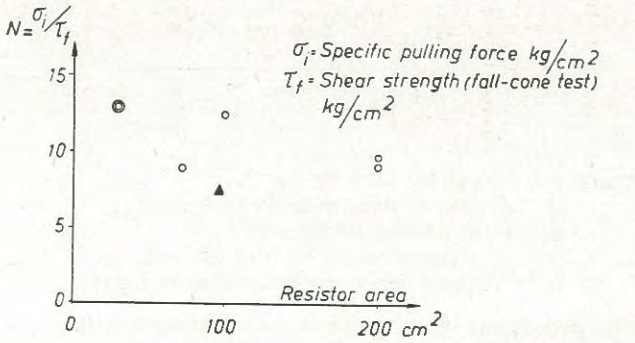

Fig. 12 Early calibration of Iskymeter (Kjellman and Liljedahl, 1939-1941).
Etalonnage de l'iskymètre à l'origine (Kjellman et Liljedahl, en 1939-1941).

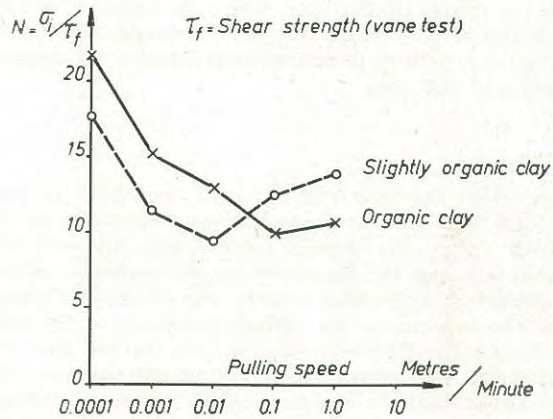

Fig. 13 Influence of clay and pulling speed (Jakobson and Wager, 1955).
Influence de la nature de l'argile et de la vitesse de traction (Jakobson et Wager, en 1955).

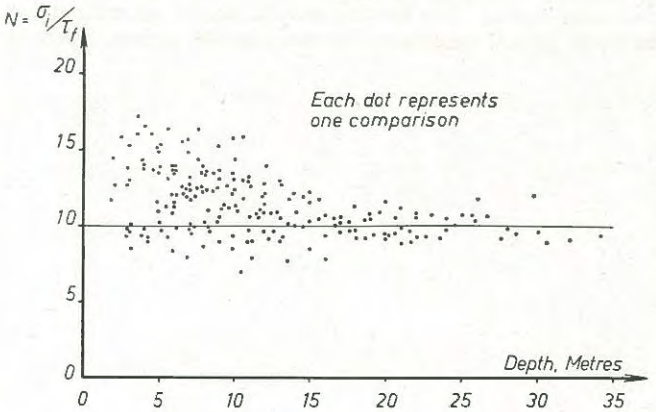

Fig. 14 Uncorrected Iskymeter values (Compared with Field Vane Test).
Valeurs données par l'iskymètre non corrigées (comparées avec des essais de chantier faits avec un moulinet).

a semi-empirical expression for correction of the pulling force for sensitivity and for depth. His expression, as derived mainly for the 100 sq. cm resistor body, is the following:

$$\tau_f = \frac{0{\cdot}092\ P}{\left(1+\frac{2}{S_t}\right)A} + \frac{0{\cdot}06 \cdot \gamma \cdot h \cdot \left(1-\frac{1}{S_t}\right)}{1+\frac{2}{S_t}}$$

Where P = pulling force in kg
A = area of resistor body in sq. cm
S_t = sensitivity of the clay
γ = volume weight in tons per cub. m.
h = depth below ground surface in metres.

(The dimensions were chosen to suit existing practice.)

The expression is mainly based on sliding circle calculations and considerations of shear strength reduction in relation to the sensitivity close to the resistor and below it. After aplying the formula the average scatter of results was reduced to the order $\pm$ 10 per cent.

It is possible to produce an expression for the evaluation based on the theory of plasticity, where the modulus of elasticity can also be considered. The scatter should therefore be reduced but it is difficult to determine accurately the modulus of elasticity of the soil.

Experience

The Iskymeter has been used in recent years both for preliminary and for detailed investigations, especially in the Göta River Valley. The results agree reasonably well with other rapid tests and, the Iskymeter has the particular advantage of providing continuous records. Fig 15 shows a typical diagram. The capacity under normal conditions is 3-4 holes in eight hours. The Iskymeter can be used for soft clays for depths down to 100 metres as friction against the wire rope is small and can easily be compensated for. A special problem for such great depths is the difficulty of driving the resistor vertically into the ground.

Conclusions

The continuity of both methods provides better knowledge of stratification than is possible with discontinuous sampling or in-situ testing. The written records enable an estimate to be made of soil conditions by studying the curves. There is also a considerable reduction in the number of samples required on a site.

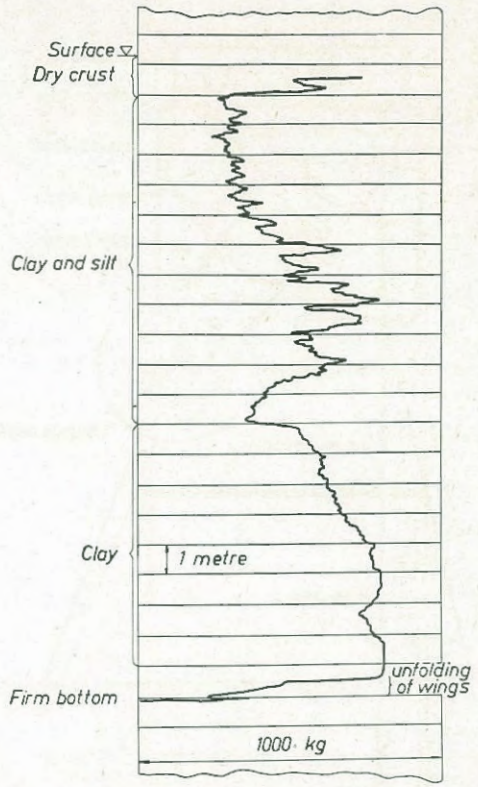

Fig. 15 Iskymeter-diagram (Göta, 1957).
Diagramme d'iskymètre (Göta, en 1957).

The diagrams are ready for reading at the exploration site. This means that the operator can make another sounding in case of dubious results and that the field work can be organised in accordance with the ground conditions. This may also entail fewer boreholes and the provision of more immediate information on the most suitable foundation methods to be adopted.

The two methods have revealed that the use of different equipments can be both rational and economical. For any site, calibration can be done by testing only a few samples.

In Situ Determination of Horizontal Ground Movements

Détermination in situ des mouvements horizontaux du sol

by T. KALLSTENIUS, Techn. Lic., Head of Mechanical Department, Swedish Geotechnical Institute
and
W. BERGAU, Dr Ing., Head of Measuring Section, Swedish Geotechnical Institute

Summary

The Swedish Geotechnical Institute has developed new inclinometers for accurate determination of horizontal ground movements. The instruments are normally applied in smooth flexible tubes installed vertically in the ground.

One purely mechanical device — the "SGI Rod Inclinometer" — is suitable for depths down to 4 metres. A second device — the "SGI Strain Gauge Inclinometer" — is used for depths down to 90 metres. This device has great accuracy due to the fact that the zero point travel of the strain gauges is eliminated through a special measuring method. Both devices also give the direction of the inclination of the flexible tube. The Strain Gauge Inclinometer permits polygon measurements starting from a firm bottom or any other bench mark. By repeated measurements, ground movements can be determined.

A third instrument — the "SGI Contact Pendulum" — consists of a pendulum in electrical contact with a remotely controlled micrometer screw. It can be left installed in the ground for a long time in order to check the changes in inclination at a given level, normally selected by previous measurements with the Strain Gauge Inclinometer. The Contact Pendulum may serve as a warning of excessive ground movements.

Sommaire

De nouveaux inclinomètres ont été mis au point à l'Institut Suédois de Géotechnique pour la mesure précise des mouvements horizontaux du sol. Ces appareils sont normalement placés dans des tubes lisses flexibles disposés verticalement dans le sol.

Un appareil purement mécanique — l'inclinomètre à tige SGI — est utilisable jusqu'à 4 m de profondeur.

Un autre appareil — l'inclinomètre à strain gages SGI — peut être employé jusqu'à 90 m de profondeur. Cet appareil est d'une grande précision, dûe notamment à ce que la dérive du zéro des strain gages est éliminée par la méthode de mesure adoptée.

Les deux appareils indiquent également la direction dans laquelle s'incline le tube flexible.

L'inclinomètre à strain gages permet de déterminer la déformée du tube flexible par des mesures en divers points, en partant de la base de ce tube si elle est fixe ou de tout autre repère. Des mesures répétées permettent de déterminer les mouvements du sol.

Un troisième appareil — le pendule à contact SGI — est constitué par un pendule qui entre en contact électrique avec une vis micrométrique commandée à distance. L'appareil peut être laissé longtemps dans le sol pour suivre les variations d'inclinaison à un niveau donné, choisi d'après les mesures faites antérieurement à l'aide de l'inclinomètre à strain gages. Le pendule à contact peut servir d'avertisseur pour déceler des mouvements du sol dépassant une certaine ampleur.

Introduction

Determination of horizontal ground movements is important in soil mechanics. In recent years many measurements of such movements have been taken all over the world.

The Swedish Geotechnical Institute in 1957 needed such measurements for a large-scale field test and for research into the kinetics leading to failure of natural slopes. The authors studied available borehole inclinometers for that purpose. Although a great variety of these are used for different purposes they could find no type which combined small diameter with high accuracy in the determination of size and horizontal direction of inclination. They therefore developed the special instruments described in the paper.

The SGI Rod Inclinometer

When, in June 1957, a large-scale consolidation test was started at Skå Edeby near Stockholm and measurement of horizontal displacements both at the ground surface and in the ground was considered essential, an available borehole inclinometer was used but failed to some extent. Another type was therefore urgently needed. Mr. A. Hallén, of the Institute's mechanical department, was put in charge of the development of a simple rod meter for shallow depths only, as it was probable that ground movements at great depths were small. This meter was soon in operation and has since been gradually improved.

Fig. 1 shows the measuring principle. A flexible tube with an internal diameter of 40-110 mm is installed in the ground and a straight rod is inserted in the tube with a flexible guide following the bends of the tube. Where the rod enters the tube it is centered by means of a disc and a spherical guide.

The inclination and length of rod between the guides determines the position of the centre of the lower guide in relation to the centre of the spherical guide. The position of the latter is determined by geodetic means in relation to a bench-mark.

The direction and the size of inclination are measured by means of an instrument mounted on the rod. The instrument has one part which can be fixed to the rod and one part which can be turned. The first part is fixed after the diopter has been directed in a chosen horizontal zero direction. Then the other part of the instrument is turned until a tangentially positioned spirit level indicates a horizontal position. That position corresponds to the inclination plane of the rod. The horizontal angle between this position and the zero direction is given by the position of an index on the turnable part in relation to a scale disc on the fixed part.

The inclination is obtained by setting a radial spirit level

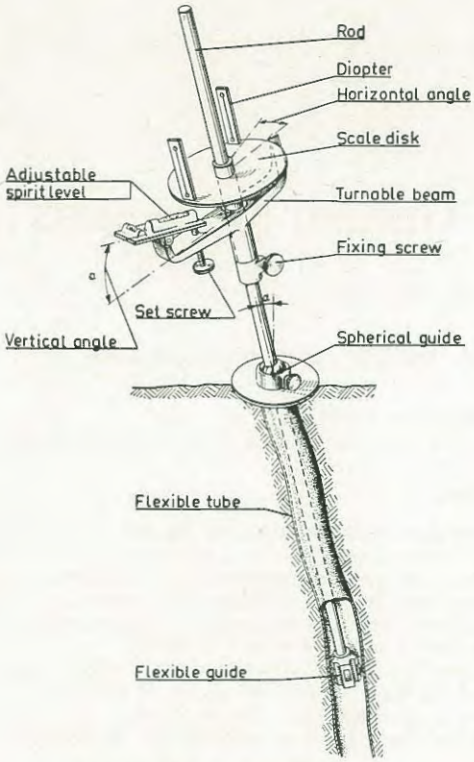

Fig. 1 Rod Inclinometer.
Inclinomètre à tige.

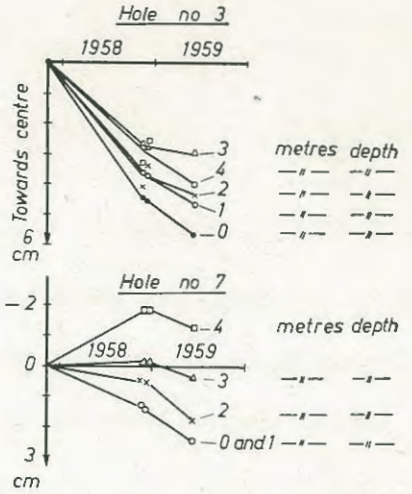

Fig. 2 Rod Inclinometer. Measurements at Skå-Edeby.
Inclinomètre à tige. Mesures faites à Skå-Edeby.

in a horizontal position by means of a set screw and reading the position either on the set screw, which in this case is a micrometer screw, or on a dial gauge (not shown in the figure).

To take a measurement the rod is inserted to different depths. For each depth three readings are taken, between each of which the rod is turned through 120 degrees. The observed scatter between these readings has averaged $\pm$ 0·35 mm deviation in horizontal direction for one metre's depth, $\pm$ 0·5 mm for two metres' depth and $\pm$ 0·9 mm for three metres'depth. At four metres' depth the scatter has hitherto increased suddenly about ten times to + 6·7 mm. The cause was an incorrect joint (as the rod had to be lengthened for that depth) but even the flexible guide can be influenced by the weight of the system (which probably also is the reason why the relatively minimum scatter was obtained for two metres' depth). These parts have now been improved.

Fig. 2 shows some measurements made over a period of two years at Skå Edeby.

The Rod Inclinometer seems to be particularly suitable for measurements on embankments and levees for depths down to 4 metres. Its main advantage is its simplicity.

The SGI-Strain-Gauge Inclinometer

The Strain-Gauge Inclinometer was primarily intended for the determination of horizontal movements in clay down to 20-30 m depths but has also been used with piles (70 m length) and for measurements in an earth dam which will have a height of 90 m when completed.

For measurements in clay a flexible tube with an inside diameter of 40 mm is installed vertically in the ground. If possible the lower end of the tube is fastened to firm bottom. That point can then provide a bench-mark for measurement of the horizontal travel of the tube. In addition the position of the upper end of the tube should, when possible, be determined on the surface. By combining a fixed lower end and a measured upper end the accuracy can be checked. Even if the positions of the ends are neglected useful information about relative soil movements is obtained from the shape of the curves.

The instrument, in its cylindrical cover, is directed by means of a spring and guiding knobs within the plastic tube. Each end of the cover is in contact with the tube wall at three points, and the axial distance between the contact points is 200 mm.

When measuring the inclination and the horizontal direction of the plastic tube at different levels the shape of the tube can be determined as a polygon. The conformity of the computed polygon to the tube centre line is dependent on the spacing of the measuring levels and on the curvature of the tube. For a tube with a continually gentle slope this spacing can be increased, whereas a tnbe with inflexion points will need closer spacing. The necessary spacing is also determined by the stiffness of the tube. A stiff tube is less sensitive to local changes and permits greater spacing while a softer tube follows the ground movements more closely and requires more measuring points.

In practice the authors usually carry out the first two series of measurements with a spacing of 0·5 m; thereafter the suitable spacing is prescribed for each tube (even with regard to economy).

The measuring principle of the inclinometer should permit determination with high accuracy of even large angles in tubes of 40 mm inside diameter.

The chosen method is based on the measurement (by electrical resistance strain gauges) of the strain in a leaf spring stressed by a weight (Fig. 3). The usually disturbing factors with strain gauge measurements (e.g. zero drift, creep, varying temperature differences between the measuring bridge and the inclinometer in the ground) do not influence the measuring result owing to the adoption of the measuring procedure that the meter is turned round in the tube. During one turn the spring will first deflect in one direction until, after a maximum deviation value (Fig. 4a) (which is indicated as a strain value at the measuring bridge), it then deflects in the opposite direction to another maximum (Fig. 4b) giving another strain value. It is the difference between these values which is calibrated against a known inclination of the instrument.

In practice the inclinometer is inserted into the plastic tube to the desired level by means of extension tubes (normally

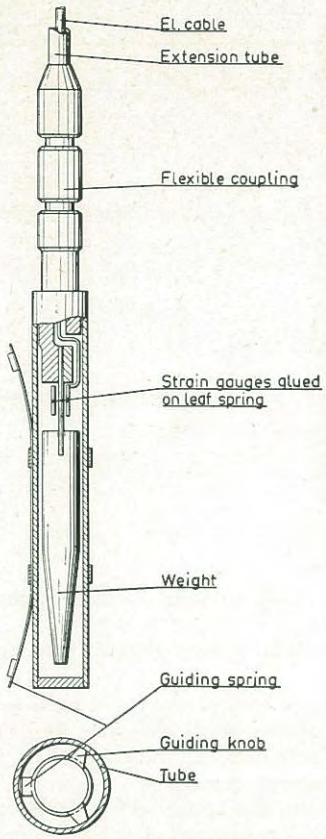

Fig. 3 Strain Gauge Inclinometer.
Inclinomètre à gages.

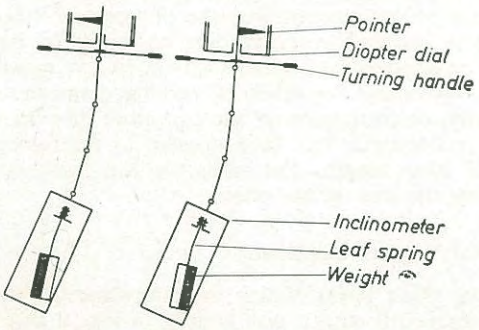

Fig. 4 Strain Gauge Inclinometer. Measuring Principle.
Inclinomètre à gages. Principe de mesure.

one metre in length) provided with flexible couplings (Fig. 5). After that a turning handle is fastened to the uppermost extension tube. The whole system is then rotated for measurement.

The direction of the plastic tube in horizontal projection at the actual level is determined by means of a diopter dial fixed in a certain position on the extension tube. All screws on the couplings and on the extension tubes are positioned along a straight line and hence the pointer of the diopter dial (Fig. 4) indicates the horizontal direction of the inclinometer when it has reached one of the positions of maximum deflection (which can be obtained from the bridge reading if the electrical cables are connected to the bridge in suitable order). The angle of horizontal direction is then read on the dial between the pointer and a line to an arbitrary chosen fixed point on the surface. The measuring accuracy of the inclinometer is dependent on the stability and freedom from

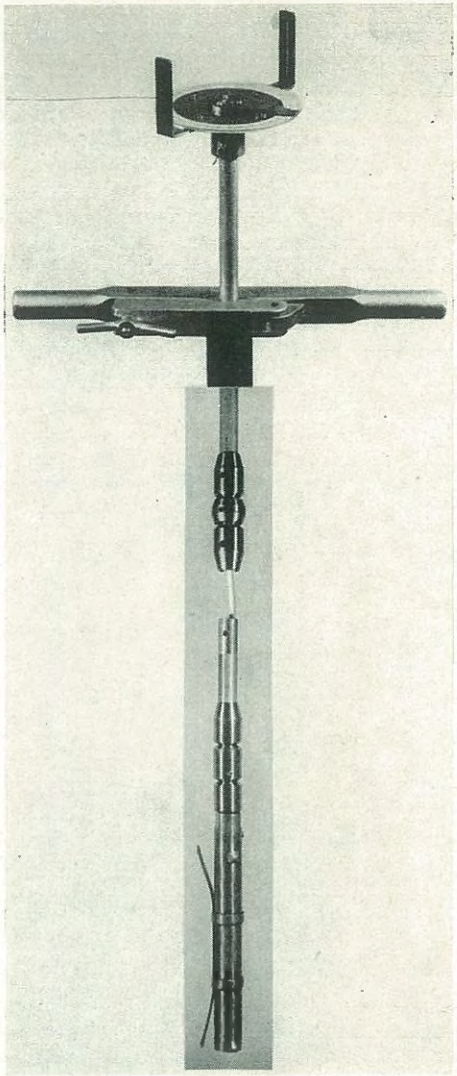

Fig. 5 Strain Gauge Inclinometer. Measuring Set Up.
Inclinomètre à gages. Equipement de mesure.

hysteresis of the leaf spring. If the allowable stress on the spring is too limited, the resistance variations in the strain gauges may be too small for a safe indication on the bridge. How personal factors may influence accuracy, especially when compensating and reading the bridge, was examined by comparative tests. Three measurements in a tube at Skå Edeby were carried out by three different staffs. The tube happened to lie in a plane and the obtained horizontal coordinates in this plane are shown in Table 1.

Table 1

Depth m	*Coordinate*		
	1st measurement mm	*2nd measurement* mm	*3rd measurement* mm
0	0	0	0
1·50	74	73	73
3·00	157	156	155
4·50	253	251	252
6·00	353	354	354
7·50	468	469	469
9·00	—	597	597

These and later field measurements by the authors have shown that the Strain-Gauge Inclinometer now has an accuracy better than $\pm$ 0·02° for inclinations below 45°.

The results of the measurements are presented in a three-dimensional coordinate system either by setting up graphically the curve of the tube, or by computing its coordinates, which is more accurate. Fig. 6 shows the results of two measurements where a certain change has occurred in the meantime. Such a method of presentation is correct but hardly examinable. When the first aim of the investigations is to determine horizontal movements it is often sufficient to establish the principal plane of movement and to report the results only in this plane in a manner that the variations against the initial position of the tube are shown. Comparison of results is furthermore facilitated when measurements are always made at the same depths.

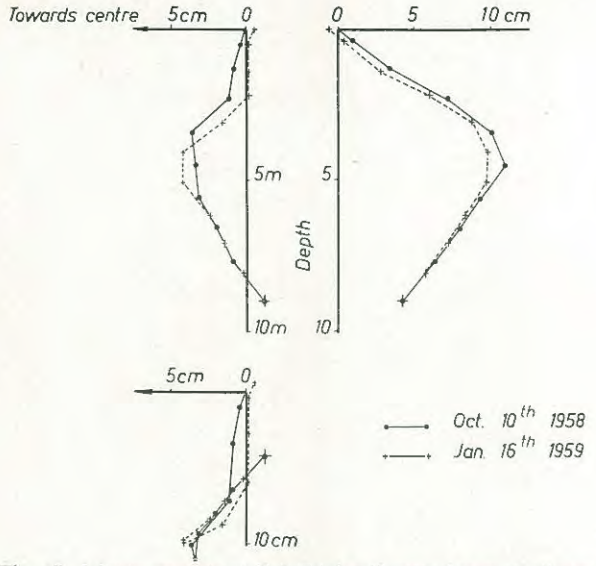

Fig. 6 Measurements at Skå-Edeby (Strain Gauge Inclinometer).
Mesures faites à Skå-Edeby (Inclinomètre à gages).

In Fig. 7 the results of measurements in a slope at the Göta River Valley are set out. The slope runs out in a tongue-like shape, and the principal plane of movement coincides with the axis of the tongue. The plastic-tube was set down through a clay stratum to a bottom layer of moraine where its conical iron tip was fixed at a depth of 17·25 metres. The position of the upper end of the tube is determined against a benchmark in the vicinity. Thus the position of the tube, determined from the fixed tip, can be checked on the surface. The first series of measurements is represented by the vertical axis, and the deviation from these initial values is indicated in the diagram. The curves reveal that lateral displacements in the soil obviously begin at a depth of about 8 m. Moreover an increasing tendency of the curves to buckle is visible. This is due to (observed) vertical settlements. When the soil settles it presses down the tube by friction thus causing small lateral deflections. By coating the tube with asphalt protected by a bandage of aluminium strips, friction between soil and tube can be reduced. Such an arrangement has been made at Skå Edeby, but for the present measurements it was considered unecessary and uneconomical. So far this simplification seems to have been acceptable.

The method of controlling the position of a vertically installed plastic tube in the ground by the Strain-Gauge Inclinometer is now used for observation purposes at different sites. For a bridge abutment extensive excavations and considerable piling work had to be carried out, and harmful movements

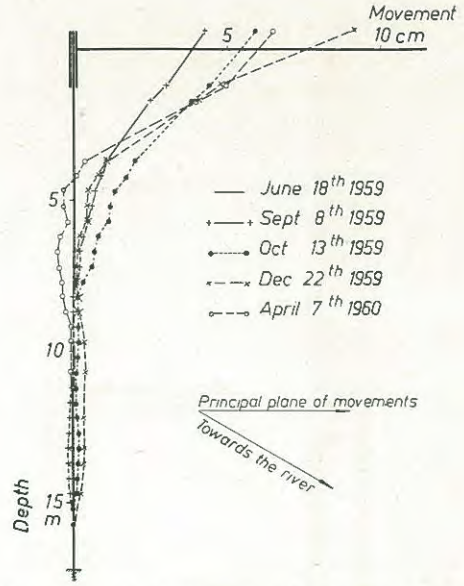

Fig. 7 Measurements at Strandbacken (Strain Gauge Inclinometer).
Mesures faites à Strandbacken (Inclinomètre à gages).

were feared. Hence two plastic tubes were installed from sea level in front of the abutment area. Both excavation and piling were reflected in the movements of the tubes. After piling the movement ceased.

Another problem has appeared in a large earth dam, where the lateral variations in a set of vertical telescopic tubes had to be determined. When completed, the dam will have a height of 90 m. The loosely jointed telescopic set (tube diameters 40 mm and 53 mm) is in the first place intended for the determination of settlements. For the purpose of measuring the change in inclination the guiding cover of the inclinometer had to be constructed in such a way as to give reliable contact of the instrument for tubes of varying diameter.

For the determination of the curvature of piles the strain-gauge inclinometer has been applied to reinforced concrete piles of 70 m length. The tubes for the inclinometer were set along the axis of the piles.

The SGI Contact Pendulum

In the Göta River Valley in southwestern Sweden slides occur frequently and it was desired to install instruments in the ground to warn against possible slides earlier than occasional observation of the ground surface can do.

The authors designed an instrument which could be left in the ground for a long time and could be operated by a non-specialist.

The chosen procedure was to install a tube as for the Strain-Gauge Inclinometer. A few consecutive measurements were then made with the Strain-Gauge Inclinometer to get a general idea as to where movements occur in the ground. Finally a long-term inclinometer is installed at the actual depth and with a horizontal orientation determined by means of the Strain-Gauge Inclinometer or otherwise.

The Contact Pendulum has been developed for such long-term purposes. In principle it is a mechanical device as shown in Fig. 8. The pendulum is hinged on ball-bearings and assumes a vertical position. A micrometer-screw can be turned by means of a thin shaft and a gear. When the screw touches an electrical contact on the pendulum, a signal is obtained above ground. The pendulum and contact are immersed in oil which provides protection against corrosion and has a damping effect on the pendulum.

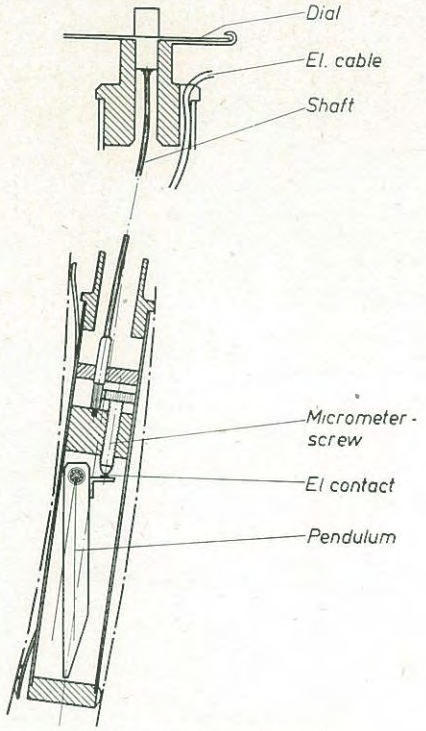

Fig. 8 Contact Pendulum.
Pendule à contact.

This damping ensures good electrical contact without noticeable deflexion of the pendulum. Care is taken to use a very weak current and never to break the contact with the current switched on. Thus great accuracy (contact travel about 1 μ) and long life of the contact is ensured.

The mircrometer screw is manipulated from above ground by means of a turning knob (provided with a dial). A 90° turn of the dial means a 0·1° corresponding change in inclination of the pendulum. Therefore the twist of the shaft — which is only a few degrees — does not influence the results.

By counting the necessary number of rotations of the dial to get a contact and comparing that number with the number of turns required when the instrument is held in a vertical position the inclination can be determined. This is, however, not the recommended procedure when checking ground movements. In such cases it is sufficient to install the Contact Pendulum in the tube and turn the dial until contact is obtained. This gives an initial position. Then the dial is turned backwards. After some time a new contact is established and the change in inclination is obtained from the difference of the readings.

A possibility (not yet applied but intended to be performed) is the application of an arrangement giving an automatic signal. One can then open the contact gap a known distance. When the inclination reaches a corresponding value a signal is obtained. If the soil in a slope is creeping at a certain rate the contact can be preset to cover the movement during a certain period of time. If the movement is accelerated a signal is obtained before the presumed time interval is ended.

Two types of contact pendulum have been made. One specimen of the ordinary type had been left in the ground for eighteen months up to the time of writing. At Skå Edeby this meter was installed 2 metres apart from a tube where measurements were performed with the Rod Inclinometer. Fig. 9 shows a comparison of the measurements. The contact pendulum has remained sensitive.

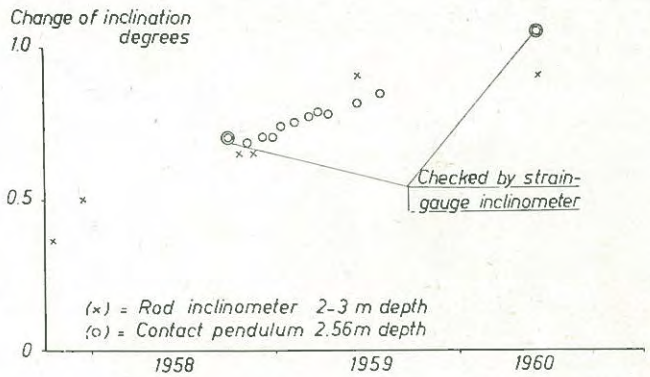

Fig. 9 Measurements at Skå-Edeby (Rod Inclinometer, Contact Pendulum).
Mesures faites à Skå-Edeby (Inclinomètre à tige et pendule à contact).

A precision pendulum has also been built with a sensitivity of about 0·002° (measuring range 0-1°). This indicates that the principle can give a high degree of accuracy.